

Ultrafast synthesis of bentonite-acrylate nanocomposite materials by UV-radiation curing

C. DECKER*, K. ZAHOUILY*, L. KELLER*, S. BENFARHI*[§], T. BENDAIKHA*[§], J. BARON[‡]

**Département de Photochimie Générale (CNRS) and ‡Laboratoire de Matériaux Minéraux (CNRS), Ecole Nationale Supérieure de Chimie de Mulhouse, 3 rue Werner, 68200 Mulhouse, France*

Nanocomposite materials made of silicate platelets randomly dispersed in a crosslinked polyurethane-acrylate have been readily produced by photoinitiated polymerization. The mineral filler (bentonite) was treated by an ammonium salt or an acrylated amine to make it organophilic and allow the acrylic resin containing a photoinitiator (aromatic ketone) to penetrate into the expanded organoclay galleries. The photoinitiated crosslinking polymerization reaction was followed in real time by infrared spectroscopy and shown to proceed extensively (>95% conversion) within a few seconds of UV-irradiation. The flat X-ray diffraction spectra recorded with the UV-cured material shows that the layered silicate has been completely exfoliated, thus demonstrating that a nanocomposite material has well been produced. This method of synthesis presents the distinct advantages associated with the UV-curing technology, namely, a solvent-free formulation undergoing ultrafast polymerization at ambient temperature in the presence of air.

© 2002 Kluwer Academic Publishers

1. Introduction

Nanocomposites are a new class of particle-filled polymers where the dimensions of the dispersed particles are in the nanometer range [1]. These materials are usually obtained by intercalation of a polymer (or a monomer subsequently polymerized) inside the galleries of the layered host crystals consisting most often of layered silicates such as clay. There has been a growing interest in nanocomposites which, because of the well-dispersed nanometer-size particles and the good compatibility between the organic matrix and the mineral filler, exhibit superior mechanical, thermal, optical and barrier properties than conventional-scaled composite materials [2]. Nanocomposites formation requires a full exfoliation in the host polymer matrix of the one nanometer thick clay platelets which must therefore be made organophilic by an adequate pre-treatment, usually by exchange of the alkali cations through ammonium salts [3]. Since the first report in 1961 by Blumstein [4] on the synthesis of vinyl polymer–montmorillonite nanocomposites, a large number of studies have been reported, mainly in the past 10 years, on the preparation, properties and applications of polymer-layered silicate nanocomposites [5–11]. The subject has been thoroughly covered recently by Alexandre and Dubois in a comprehensive survey [1].

Most of the nanocomposite materials are based on linear polymers having each their distinct mechanical properties, e.g., polyamides [2, 12], polyolefins [6, 13,

14], polystyrene [15, 16] and polyurethanes [17]. Because all these polymers are soluble in the organic solvents, the nanocomposites made from them show a poor chemical resistance. Although the thermal stability of nanocomposites is generally higher than that of the parent polymer, the improvement is yet limited. Moreover, the mineral filler is usually incorporated into the melted polymer which must be kept in the liquid state for some time to ensure adequate swelling and intercalation into (or exfoliation of) the clay platelets. Thermo-degradation may occur during this treatment, depending on the temperature and the environment (oxygen, moisture, etc), thus affecting the composite heat stability.

This drawback is avoided with the solvent-based processing, which yet releases large amounts of volatile organic compounds and needs a thorough drying to eliminate the residual solvent trapped between the clay platelets. The chemical and heat resistance of nanocomposite materials can be markedly enhanced by using a binder undergoing *in situ* crosslinking, like with epoxy-based thermosetting polymers [18–20].

The objective of this work was to produce highly resistant nanocomposite materials by a fast and environment friendly process. The basic idea was to use a solvent-free UV-curable resin and introduce a nano-scale filler to improve its properties. *In situ* intercalative polymerization proved to be the most appropriate technique to prepare polymer layered silicate

[§]On leave from the University of Batna (Algeria).

nanocomposites, by simple UV irradiation of the layered silicate swollen within the liquid monomer containing a photoinitiator. By contrast to conventional composite materials which are opaque, nanocomposites are essentially transparent to light, thus allowing a deep through-thickness cure of relatively thick samples (up to a few millimeters) to be achieved by UV irradiation. UV-curable resins are made of multifunctional monomers and oligomers, mainly acrylates, which generate upon radical induced polymerization in a tight tridimensional polymer network.

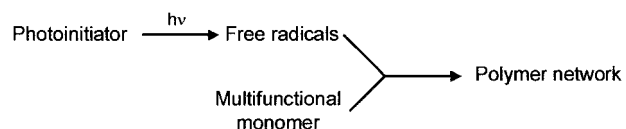
Using UV-radiation to initiate the crosslinking polymerization of the multifunctional monomer has a number of advantages [21]:

- a solvent free-formulation, with essentially no emission of volatile organic compounds;
- a fine control of the swelling time to ensure a perfect interpenetration of the resin into the lattice layers of the clay mineral;
- operations at ambient temperature in the presence of air;
- a precise control of the polymerization onset, simply by switching on the light;
- an ultrafast curing by using the highly reactive acrylate-based resins and adequate photoinitiators;
- a fine control of the polymerization rate in a large domain, simply by controlling the light intensity;
- a large range of mechanical properties, from soft and flexible composite materials to hard organic glasses, by a proper choice of the telechelic oligomer;
- the production of cured polymers very resistant to heat and chemicals because of their high crosslink density.

While nanocomposite materials have been recently produced by electron-beam curing [22] or by γ irradiation [23], only scant information is found in the literature on UV-cured nanocomposites [24–29]. Nanocomposite adhesives for applications in integrated optics have been produced by UV-curing of an epoxy-based resin containing up to 20 wt% of nanonized silica particle [26]. The abrasion and scratching resistance of UV-cured coatings was found to be greatly improved by incorporation into the acrylic matrix of acrylate functionalized colloidal silica [24, 25, 28]. In a very recent work, Huimin *et al.* [29] produced polymer/montmorillonite nanocomposite materials by photopolymerization of either methyl/methacrylate or a m-cresol resin intercalated into the layers of the clay mineral. However, besides the very slow cure which makes this process ill-suited for industrial use, the nanocomposites obtained exhibit a deep color, thus limiting the penetration of UV light and therefore the thickness of the cured sample.

Recently, we have obtained much better performance with respect to both cure speed and material properties by achieving a complete defoliation of the filler and by using a crosslinkable polyurethane-acrylate binder [27]. The study reported here has been focused mainly on the optimization of the pre-treatment of the clay min-

eral to render it completely organophilic, and on the kinetic aspect of the polymerization reaction to speed up the process and make it well suited for industrial applications. Exfoliation of the clay platelets, demonstrated by X ray spectroscopy, was achieved by exchanging the intergallery sodium cations of bentonite for alkylammonium cations, thus making the mineral filler compatible with the organic resin. The photoinitiated polymerization of a multifunctional monomer, which leads to a highly crosslinked polymer, can be represented schematically as follows:



The disappearance of the reactive function, e.g., the acrylate double bonds, was followed in real-time and quantitatively by infrared spectroscopy to evaluate both the formulation reactivity and the final cure extent of the nanocomposite material thus obtained.

2. Experimental

2.1. Materials

The UV-curable resin was made of four components. An acrylate end-capped polyurethane (Ebecryl 284 from UCB) was used as telechelic oligomer ($M = 1200$ g). To reduce the formulation viscosity down to 500 mPas, a reactive diluent was added at a weight concentration of 25% (hexanediol diacrylate from UCB). A combination of two photoinitiators, Darocur 1173 (2 wt%) and Irgacure 819 (1 wt%) from Ciba Specialty Chemicals, was chosen to achieve both surface and deep through cure, respectively. The fast photobleaching of the bisacylphosphine oxide (Irgacure 819) allows the incident radiation to penetrate progressively deeper into the sample and thus promote a frontal polymerization process [30].

The mineral filler selected to obtain a nanocomposite material was a natural clay from Algeria (Bentonite, BNT) which was shown by X ray diffraction to be of a high purity grade. After being made organophilic by an appropriate treatment (see below), organic bentonite (OBNT) was dispersed into the UV-curable resin at a maximum concentration of 7 wt%. To obtain a stable suspension, the mixture was exposed to ultrasounds (Bransonic 2250) for 7 h at 50°C, in the dark to prevent any premature polymerization.

2.2. Irradiation

Two types of UV irradiation equipments were used to perform a high-speed curing of the nanocomposite formulation. The first one was a Minicure set up from IST equipped with a medium pressure mercury lamp (electrical power of 80 W/cm) and a semi-elliptic reflector. It was operated at a belt speed of 5 m/min, which corresponds to an exposure time of 1 s per pass under the lamp. The maximum UV-light intensity at the sample position was measured by radiometry (International Light radiometer IL-390) to be 5.6 kW m⁻²

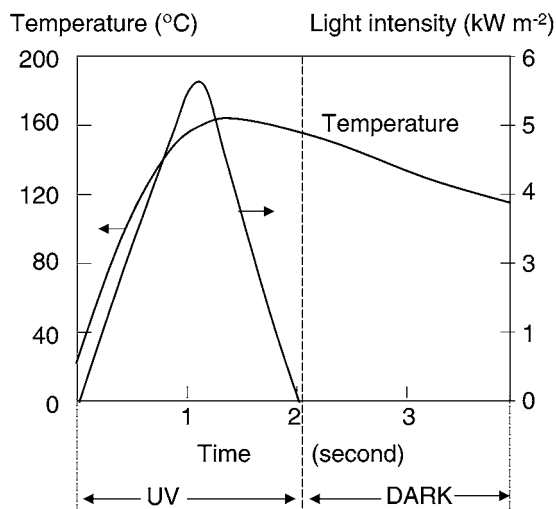


Figure 1 Temperature and light intensity profiles recorded during on-line UV-curing of an acrylate resin. Film thickness: 400 μm .

in the 250–400 nm wavelength range covered by this radiometer. The UV-curable resin was deposited on a glass plate at thicknesses up to 2 mm and exposed to UV radiation by 4 successive passes. These short exposures, followed each by a 1 s post-polymerization [31], proved to be enough to transform the liquid resin into a hard and solid material.

A second type of irradiation device (Novacure from EFOS), equipped with a mercury lamp and an optical guide, was used for the kinetic analysis of the polymerization by real time infrared (RTIR) spectroscopy [32]. The light intensity at the sample position could be varied between 0.15 and 4.0 kW m^{-2} .

All the irradiation experiments have been carried out at ambient temperature in the presence of air. It should be noted that, because of the exothermicity of the polymerization reaction, the sample temperature can still rise up to fairly high values, specially in thick samples [33]. Fig. 1 shows a typical temperature profile recorded in a 400 μm thick sample passing under the IST lamp at a speed of 5 m/min. A more complete polymerization will thus be achieved as a result of the increased molecular mobility, specially in the ultimate stage of the curing process.

2.3. Analysis

2.3.1. Monitoring of the photopolymerization by RTIR spectroscopy

A Fourier transformed infrared spectrophotometer (Bruker IFG-66), equipped with a MCT detector, was employed to monitor continuously the decrease upon UV exposure of the IR band at 810 cm^{-1} of the acrylate double bond ($\text{CH}_2=\text{CH}$ twisting). Up to 50 IR spectra were recorded per second, thus allowing an accurate monitoring of high-speed reactions. Fig. 2 shows a typical IR spectrum of the UV-curable resin and its variation upon UV exposure. It should be noted that the presence of the OBNT filler is not interfering with the acrylate IR band. The 30 μm thick sample, coated onto a KBr crystal, was exposed simultaneously to the

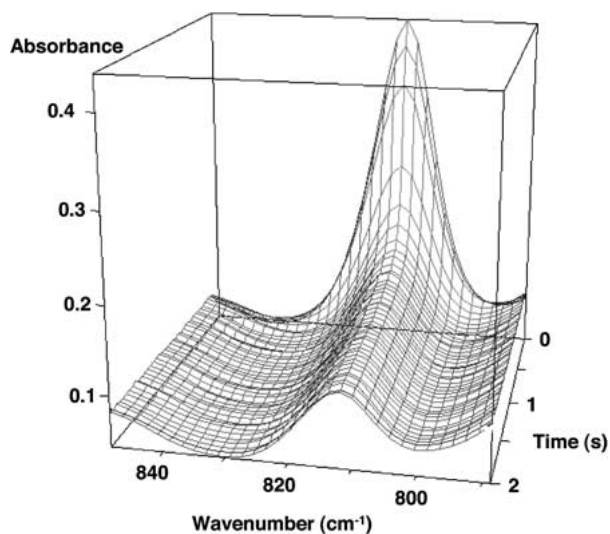


Figure 2 Infrared spectra of a diacrylate monomer before and after various exposure times up to 2 s.

UV beam that induces the polymerization of the acrylate resin and to the IR beam which analyzes *in situ* the resulting chemical modifications. Conversion *versus* time curves were directly recorded by following the disappearance of the acrylate double bond. In this kinetic study, the light intensity at the sample position, which can be varied in a broad range, was set at 1 kW m^{-2} .

2.3.2. Characterization by X-ray diffraction spectroscopy

Powder X-ray diffraction patterns of natural bentonite (BNT) and modified bentonite (OBNT) have been recorded by means of a PX-ray diffractometer (Philips PW 1800). The Cu $K\alpha$ radiation (LFF tube 35 kV, 50 mA) was selected for the analysis, by operating with an automatic divergence slit (irradiated sample length of 10 mm), a graphite monochromator and an APD 1700 version 4.0 software. For the characterization of the UV-cured nanocomposite, a 2 mm thick disk of 24 mm diameter having a very smooth surface was produced by a 4 s UV exposure and analyzed directly by X-ray diffraction. The distance between layers (d_{001}) was calculated by using the Bragg equation, $2d \sin \theta = n\lambda$, where λ is the wavelength of the incident X ray beam, n an integer and θ the angle of incidence.

3. Results and discussion

3.1. Organoclay preparation

To obtain a true nanocomposite material, it is essential that the 1 nm thick mineral platelets be uniformly dispersed within the polymer matrix. This can only be achieved if the hydrophilic clay is made organophilic so as to allow the acrylate monomer to penetrate within the silica layers. In natural clay, bentonite or montmorillonite, a central octahedral sheet of alumina or magnesia is fused by the tip to two external silica tetrahedrons [1]. These layers organize themselves to form stacks separated by galleries and contain negative charges due to isomorphic substitution (e.g., Al^{3+} by Mg^{2+}). They

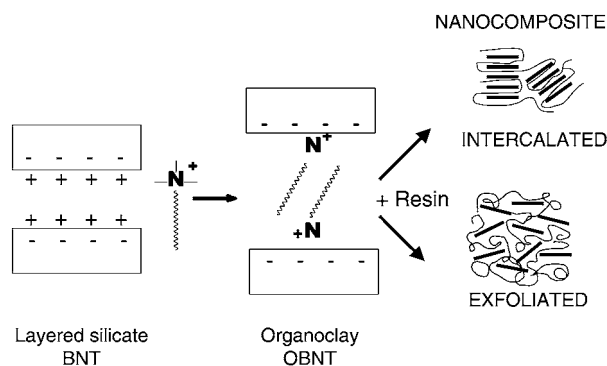


Figure 3 Preparation of the organoclay by cation exchange, followed by its dispersion in the UV-curable resin.

are counterbalanced by alkali cations (Na^+ or Ca^{++}) situated in the interlayer. Exchanging these hydrated cations by cationic surfactants, such as alkylammonium salts, will render the clay organophilic and therefore compatible with organic molecules. Depending on whether the lamella structure is preserved or not upon dispersion into the UV-curable resin, one will obtain an intercalated nanocomposite or an exfoliated nanocomposite, as shown schematically in Fig. 3.

An alkylammonium salt with a long alkyl chain (hexadecyltrimethylammonium chloride from Aldrich) was selected as surfactant to widen sufficiently the interlayer and allow the resin to penetrate into the clay galleries. To prepare the organoclay, bentonite was treated with this salt according to the procedure described in previous work [34, 35]. Hexadecyltrimethylammonium chloride (1.25 g) was dissolved in distilled water ($65 \times 10^{-6} \text{ m}^3$) containing 10^{-6} m^3 of concentrated hydrochloric acid ($3.9 \times 10^{-3} \text{ mol}$). The mixture was stirred at 80°C during 30 minutes until a clear solution was obtained, thus indicating a perfect dissolution of the ammonium salt. Bentonite (3.25 g) was added to this solution and the stirring was continued for another 3 hours. The white precipitate formed was recovered by filtration and dispersed in hot distilled water by mechanical stirring during 1 hour. The latter process was repeated twice to get a perfectly clean organoclay. The final precipitate was thoroughly dried in an oven at 80°C for 24 h to obtain the organophilic bentonite (OBNT) dispersible in the acrylic resin.

The same procedure was followed by using an acrylated amine as cationic surfactant (CN-550 from Cray-Valley), except that this compound was initially dissolved in acetone. Despite its shorter chain which may cause a smaller widening of the interlayer than with the ammonium salt, this surfactant is still of interest in that it will also work as a monomer and thus participate in the photopolymerization reaction. Once they have penetrated inside the galleries, the organic cations can adopt different orientations, depending on their chain length and on the clay charge density.

X-ray diffraction spectroscopy was used to evaluate the efficiency of the organophilic treatment and quantify the widening of the clay galleries. For the unmodified bentonite, the diffraction pattern shows a maximum for the (001) plane peak at a 2θ angle of 7.1° , which corresponds to an interlamellar spacing of 1.24 nm (Fig. 4),

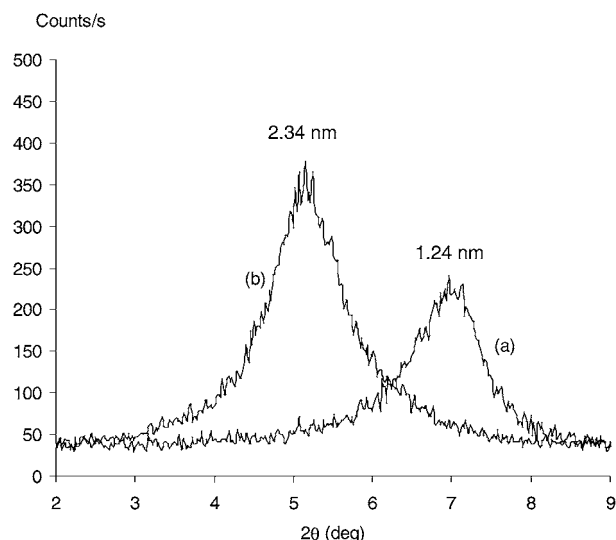


Figure 4 X-ray diffraction patterns of natural bentonite BNT (a) and the organo-clay OBNT treated by an alkylammonium salt (b). Numbers refer to the interlamellar spacing.

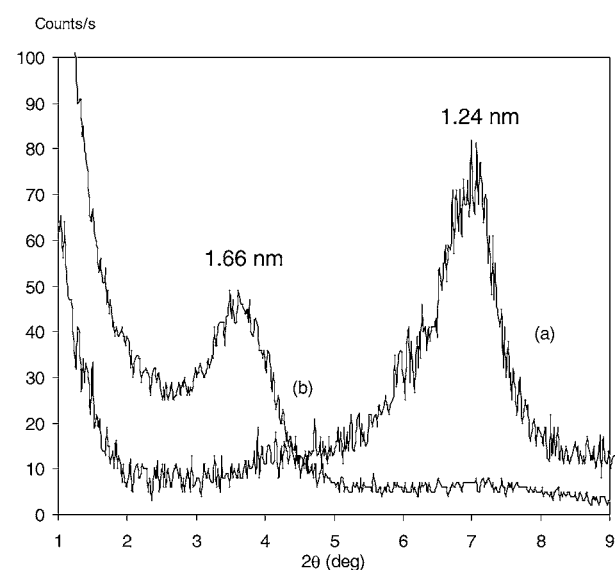


Figure 5 X-ray diffraction patterns of natural bentonite BNT (a) and the organo-clay (OBNT) treated by an acrylated amine (b). Numbers refer to the interlamellar spacing.

in good agreement with previous observations [1, 29]. For the sample treated with the ammonium salt, the diffraction peak is shifted towards lower angle values, which indicates that the distance between the clay layers has indeed increased. According to the Bragg equation, it has almost doubled to 2.34 nm, with the alkylammonium ions adopting possibly a lateral bilayer structure [36].

A similar behavior was observed with the bentonite treated by an acrylated amine, except that the interlayer spacing was growing here to only 1.66 nm, as calculated from the X-ray pattern (Fig. 5). This trend was actually expected owing to the shorter alkyl chain of the acrylated amine. Given the 33% increase only of the interlayer distance, it is likely that the short intercalated chains have adopted here a more disordered lateral monolayer arrangement.

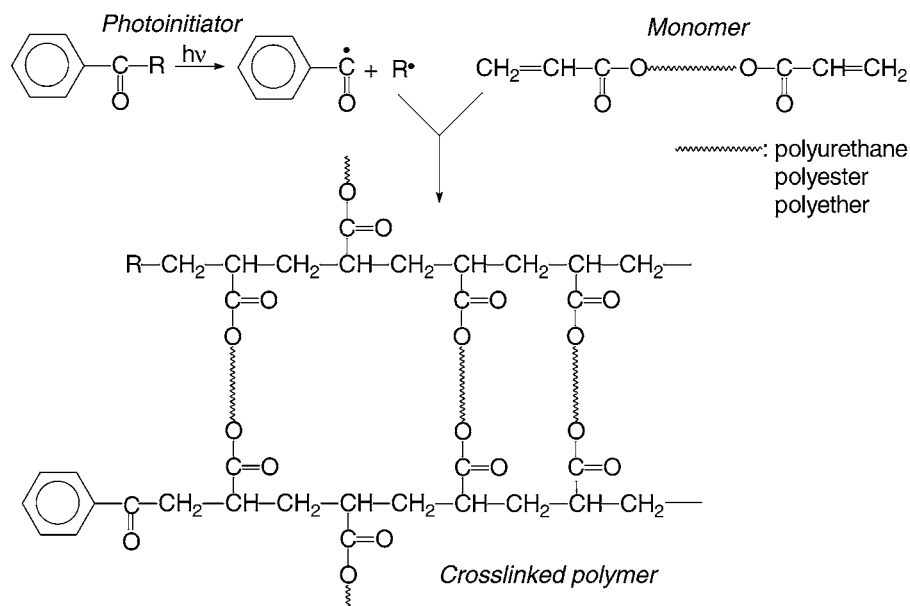


Chart 1 Reaction scheme of the photoinitiated polymerization of a diacrylate monomer.

3.2. Synthesis of nanocomposites by photopolymerization

The UV-curable resin used in this study was previously shown to polymerize rapidly and extensively upon UV-irradiation, with formation of a tight tridimensional polymer network. The photoinitiated crosslinking polymerization of a diacrylate monomer is represented schematically in Chart 1. The crosslink density of the fully cured polymer was calculated to be 3.3 mol kg^{-1} , which corresponds to an average molecular weight between branch points of 300 g.

The organoclay powder was introduced in the UV-curable resin at a weight concentration of 7%. It was homogeneously dispersed by ultrasonication for 7 hours at 50°C to allow the resin to penetrate into the clay galleries. The formulation was found to be stable upon storage in the dark at ambient temperature, the settling of the clay particles being observed only after several days. A 5 minute ultrasound treatment was sufficient to restore a homogeneous dispersion.

An important issue in this new method of preparing nanocomposite materials was to determine whether the presence of the mineral filler was affecting the polymerization kinetics, with respect to the reaction rate and the cure extent. Therefore, UV-curing experiments were performed on both the nanocomposite formulation and a reference sample containing no filler.

The polymerization reaction was followed in real time by monitoring the disappearance upon UV exposure of the IR band at 810 cm^{-1} characteristic of the acrylate double bond. Fig. 6 shows the conversion *versus* time curves recorded for the nanocomposite and reference formulations exposed to UV light at an intensity of 1 kW m^{-2} in the presence of air. The polymerization proceeds initially very fast (50% conversion within 0.3 s), and is not affected at all by the presence of the mineral filler which is not acting as a radical scavenger. The similarity between the polymerization profiles of the clear resin and the filled resin also indicates that the penetration of UV radiation into the

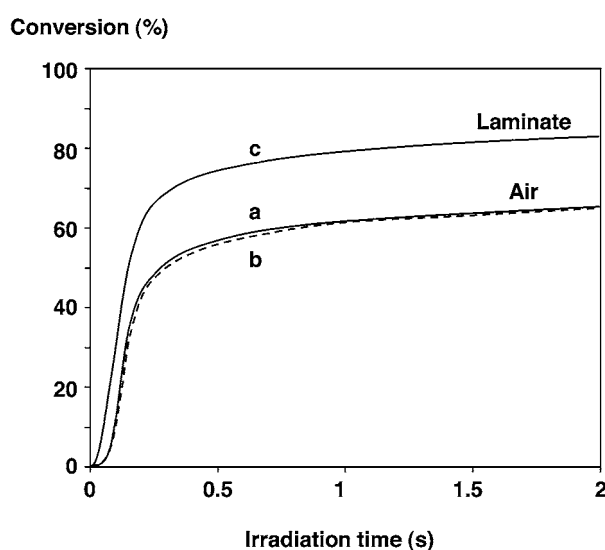
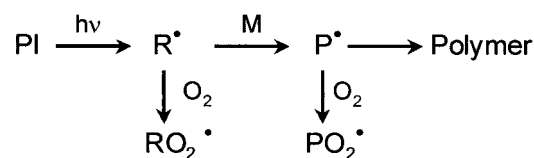


Figure 6 Polymerization profiles recorded by RTIR spectroscopy upon UV exposure of a diacrylate monomer either neat (a), or as a nanocomposite with OBNT (b), in the presence of air, or under oxygen diffusion-free conditions (c). Light intensity: 1 kW m^{-2} .

$25 \mu\text{m}$ thick sample is not reduced significantly by the presence of the organoclay.

After a 1 s UV-irradiation, the acrylate conversion reaches 60% and the polymerization is levelling off in both samples. This is due to the well known inhibitory effect of atmospheric oxygen on the radical induced polymerization of acrylates [37]:



When the sample was exposed to UV-radiation under oxygen diffusion-free conditions (laminated), the curing reaction was found to proceed faster and more extensively, as shown in Fig. 6. The polymerization was

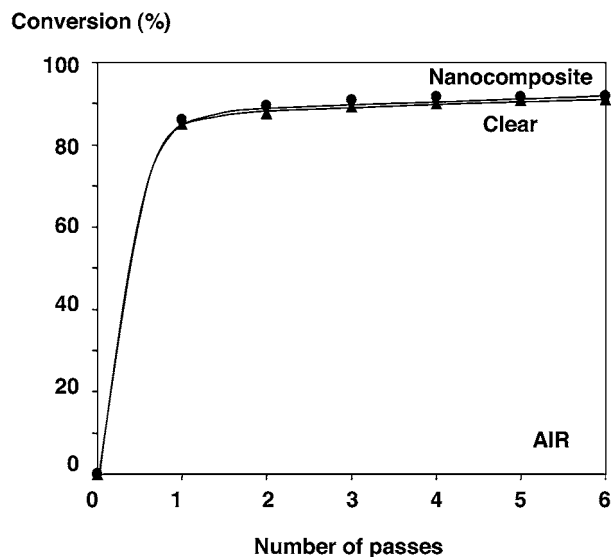


Figure 7 On-line UV-curing in the presence of air of a diacrylate monomer, with and without OBNT (7 wt%). Light intensity: 5.6 kW m^{-2} . Belt speed: 60 m/min.

still levelling off at a conversion of about 80%. The uncomplete curing is due here to molecular mobility restrictions brought upon by the liquid to solid phase change. Once the glass transition temperature of the UV-cured polymer reaches the sample temperature, the reaction stops because the polymerization can not proceed in the glassy state. Therefore there remains a certain amount of unreacted acrylate double bonds in the UV-cured nanocomposite (about 20%), even after prolonged UV exposure. Complete polymerization of the acrylate double bonds was achieved by performing the UV-irradiation at 80°C , a temperature close to the T_g of the fully cured polymer.

These photopolymerization experiments have been repeated by working under irradiation conditions comparable to those found in an industrial environment, i.e., on line processing of large samples under intense illumination in the presence of air. The cure extent of the $50 \mu\text{m}$ thick sample was evaluated by FTIR spectroscopy after repeated UV exposures. It can be seen in Fig. 7 that a 100 ms exposure (belt speed of 60 m/min) is already sufficient to obtain a solid nanocomposite material, which was deep through cured by an additional 0.25 s exposure. Oxygen inhibition is less pronounced here because of the higher intensity of the UV light (6 kW m^{-2}) and the shorter exposure time during which air can diffuse into the sample. A more complete polymerization (over 90% conversion) was achieved under those conditions, because of the increased temperature of the sample undergoing such ultrafast polymerization. It should be noted that the unreacted acrylate double bonds are bounded to the polymer network and are not extractable by solvents. Nearly complete polymerization was achieved by performing the UV-irradiation at 80°C . For further X-ray diffraction analysis, up to 2 mm thick samples were readily cured on this UV-line by operating at a web speed of 5 m/min and by passing each side of the sample twice under the UV lamp. Such photo-nanocomposites can be polymerized to the heart because the photoinitiator undergoes a rapid bleaching upon UV exposure, thus allowing the incident radiation

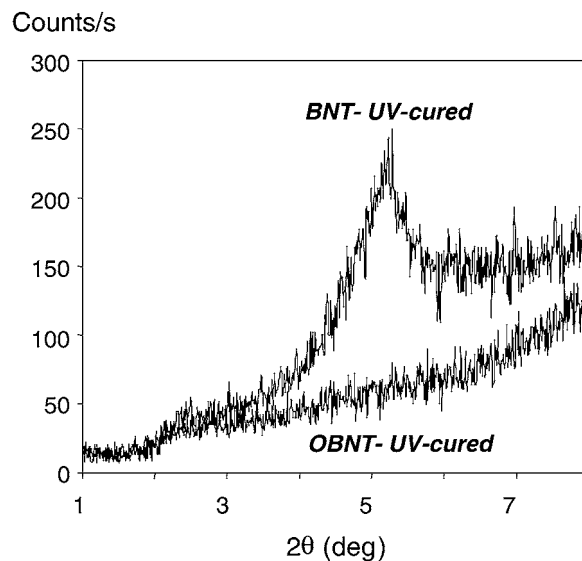


Figure 8 X-ray diffraction patterns of the UV-cured acrylate nanocomposite with OBNT and of the microcomposite with untreated BNT.

to penetrate progressively deeper into the sample and promote a frontal polymerization [30, 38].

In another series of experiments, we have tried to obtain nanocomposites by starting with a UV-curable water-based acrylate resin (Laromer PE-55 W from BASF). The polyester-acrylate emulsion containing a water soluble photoinitiator (Darocur 1173) and the organoclay (5 wt%) was first dried at 80°C during 5 minutes. The $30 \mu\text{m}$ dry film was then exposed to UV-radiation at that temperature to achieve a most complete polymerization. A single pass under the lamp at a speed of 20 m/min (0.3 s UV exposure), proved to be sufficient to polymerize 96% of the acrylate double bonds and obtain a nanocomposite material totally insoluble in water and in the organic solvents.

One of the key issues in this work was to demonstrate that exfoliation of the organoclay has really occurred upon dispersion in the acrylate resin, in order to ensure that the UV-cured material is indeed a true nanocomposite. Fig. 8 shows the X-ray diffraction pattern of the UV-cured nanocomposite based on OBNT, in comparison to the UV-cured microcomposite based on untreated BNT where exfoliation does not occur. The absence of any Bragg diffraction peak in the sample filled with the organoclay clearly indicates that the regular structure of the clay layers has been totally lost upon dispersion and polymerization of the acrylate resin. This means that exfoliation has indeed occurred quite effectively and that the 1 nm thick silicate platelets are randomly distributed within the polymer matrix. A similar behavior was observed in the polymer material containing the amine-acrylate treated organoclay.

Another experimental result arguing in favor of an effective exfoliation of the clay layers is the observed increase of transparency of the nanocomposite, compared to the microcomposite obtained with the untreated bentonite. Fig. 9 shows the UV-visible transmission spectra of $24 \mu\text{m}$ thick films with and without organoclay or mineral clay. In the non-exfoliated microcomposite, light scattering by the microparticles is more important than in the nanocomposite where the

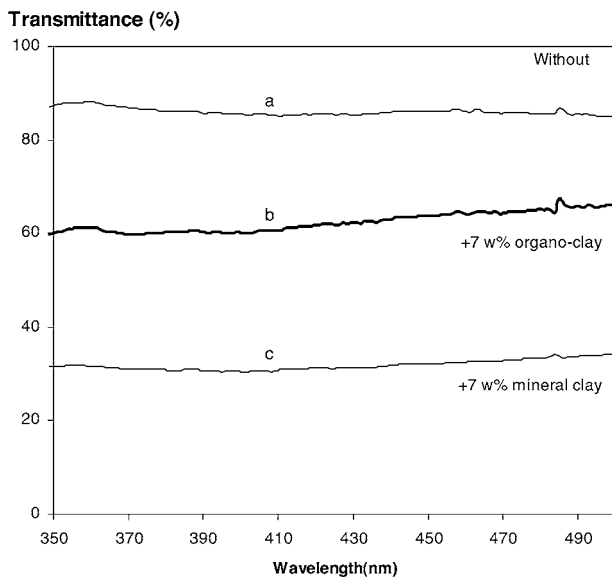


Figure 9 Transmission spectra in the visible range of a UV-cured diacrylate monomer: neat (a), as a nanocomposite with OBNT (b), as microcomposite with BNT (c).

size of the clay platelets is significantly reduced. More transparent samples could be obtained by reducing the dimensions of the mineral particles down to 50 nm, like for the colloid silica/acrylate nanocomposites which were found to be as transparent as the UV-cured clear coating [24].

According to morphology and rheology investigations, such *in situ* generated anisotropic nanoparticles assemble to form a skeleton like superstructure, which is considered to account for the enhanced properties [20, 39]. One can therefore expect such true nanocomposites, easily prepared by UV-curing, to exhibit higher stiffness and strength, a greater thermal resistance and improved gas barrier properties, as typically found in this kind of material [1]. Such study will be reported in a forthcoming article.

4. Conclusion

There is a growing interest today in nanocomposites because of the superior properties of this type of material. It has been shown here that layered silicate-based nanocomposites can be produced within seconds at ambient temperature by UV-irradiation of a multifunctional acrylate resin filled with *in situ* formed nanosilicate platelets. The layered silicates have first to be made organophilic by exchange of the intergallery sodium cations of bentonite for alkylammonium cations, in order to improve their compatibility with the monomer. Both the widening of the organoclay galleries and the complete exfoliation upon dispersion in a UV-curable acrylate resin were demonstrated by X-ray diffraction spectroscopy. A short exposure to intense UV radiation is sufficient to induce the crosslinking polymerization and obtain a hard and insoluble material containing essentially no residual monomer.

In these UV-cured nanocomposites, 1 nm thick silicate layers are randomly dispersed within the polymer matrix to form a skeleton like superstructure. This ex-

plains why a significant improvement in the polymer properties can be achieved already at low filler content. Such performance, together with a cost-effective processing of a cheap resin, are key factors for the success of these newly developed photopolymer nanocomposites. It should be emphasized that the UV-curing technology used in this study is not restricted to layered silicate-based nanocomposites and can be extended to other types of layered nanoparticles, such as superconductive nanofillers [40] and magnetic particles [41, 42] which can also be exfoliated and occluded into a polymer matrix.

References

1. M. ALEXANDRE and P. DUBOIS, *Mater. Sci. En.* **28** (2000) 1.
2. Y. KOJIMA, A. USUKI, M. KAWASUMI, A. OKADA, Y. FUKUSHIMA, T. KARAUCHI and O. KAMAGAITO, *J. Mater. Res.* **6** (1993) 1185.
3. P. C. LE BARON, Z. WANG and T. J. PINNAVAIA, *Appl. Clay Sci.* **15** (1999) 11.
4. A. BLUMSTEIN, *Bull. Soc. Chim.* (1961) 899.
5. Y. FUKUSHIMA and S. INAGAKI, *J. Inclusion Phenom.* **5** (1987) 473.
6. Q. ZHANG, Q. FU, L. JIANG and Y. LEI, *Polym. Intern.* **49** (2000) 1561.
7. R. A. VAIA and E. P. GIANNELIS, *Macromolecules* **30** (1997) 7990 and 8000.
8. P. REICHERT, J. KRESSLER, R. MÜLHAUPT and G. STÖPPELMANN *Acta. Polym.* **49** (1998) 116.
9. C. LAGALY, *Appl. Clay Sci.* **15** (1990) 1.
10. K. A. CARRADO, *ibid.* **17** (2000) 1.
11. J. W. GILMAN, C. L. JACKSON, A. B. MORGAN, R. HARRIS, E. MANIAR, E. P. GIANNELIS, M. WUTHERNOW, D. HILTON and S. PHILIPS, *Chem. Mater.* **12** (2000) 1866.
12. Y. FUKUSHIMA, A. OKADA, M. KAWASUMI, T. KURAUCHI and O. KAMIGAITO, *Clay Mineral* **23** (1988) 27.
13. M. KATO, A. USUKI and A. OKADA, *J. Appl. Polym. Sci.* **66** (1997) 1781.
14. P. DUBOIS, J. ALEXANDRE, F. HINDRYCKS and R. JEROME *J. Macromol. Sci.* **C38** (1998) 511.
15. A. AKELAH and A. MOET, *J. Mater. Sci.* **31** (1996) 1064.
16. J. G. DOH and I. CHO, *Polym. Bull* **41** (1998) 511.
17. Z. WANG and T. J. PINNAVAIA, *Chem. Mater.* **10** (1998) 3769.
18. P. B. MESSERSMITH and E. P. GIANNELIS, *ibid.* **6** (1994) 1719.
19. T. LAN and T. J. PINNAVAIA, *ibid.* **6** (1994) 2216.
20. C. ZILY, R. MÜLHAUPT and J. FINTER, *Macromol. Chem. Phys.* **200** (1999) 661.
21. C. DECKER, *Progr. Polym. Sci.* **21** (1996) 1319.
22. H. J. GLÄSEL, E. HARTMAN, R. MEHNERT, D. HIRSCH, R. BÜTTCHER and J. HORMES, *Nucl. Instr. Mat. Phys. Research B* **151** (1999) 200.
23. X. XU, Y. YIN, X. GE, H. WU and Z. ZANG, *Mater. Lett.* **37** (1998) 354.
24. C. DECKER, *Chimia* **47** (1993) 378.
25. M. MISRA, A. GUEST and M. TILLEY, *Surf. Coat. Intern.* **81** (1998) 594.
26. T. KOCH, M. MENNING and H. SCHMIDT, *Adv. Sci. Technol.* **17** (1999) 681.
27. K. ZAHOUILY, S. BENFARHI, T. BENDAIKHA, J. BARON and C. DECKER, in Proc. RadTech Europe, 2001, p. 583.
28. C. VU, O. LA FERTE and A. ERANIAN, in Proc. RadTech Europe Conf., 2001, p. 621.
29. W. HUIMIN, M. MINGHUA, J. YONGEAI, L. QINGSHAN, Z. XIACHONG and W. SHIKANG, *Polym. Intern.* **51** (2002) 7.
30. C. DECKER, *ibid.* **45** (1998) 133.
31. C. DECKER and K. MOUSSA, *Macromolecules* **22** (1989) 4455.
32. *Idem.*, *Makromol. Chem.* **189** (1988) 2381.

33. C. DECKER, D. DECKER and F. MOREL, in "Photopolymerization. Fundamentals and Applications," edited by A. B. SCRANTON, C. N. BOWMAN and R. W. PEIFFER (ACS Symp. Series 673 (Amer. Chem. Soc., Washington DC, 1997) p. 63.
34. T. LAN, P. D. KAVIRATNA and T. J. PINNAVAIA, *Chem. Mater.* **6** (1994) 573.
35. K. YANO, A. USUKI and A. OKADA, *J. Polym. Sci., Polym. Chem. Ed.* **35** (1997) 2289.
36. R. A. VAIA, R. K. TEUKOLSKY and E. P. GIANELLIS, *Chem. Mater.* **6** (1994) 1017.
37. C. DECKER and A. JENKINS, *Macromolecules* **18** (1985) 1241.
38. V. IVANOV and C. DECKER, *Polym. Intern.* **50** (2001) 113.
39. R. MÜLHAUPT, European Polymer Federation, *AIM Magazine*, (July 2001) p. 50.
40. J. H. CHOY, S. J. KWON, S. J. HWANG, Y. I. KIM and W. LEE, *J. Mater. Chem.* **9** (1999) 129.
41. V. LAGET, C. HORNICK, P. RABU and M. DRILLON, *ibid.* **9** (1999) 169.
42. J. Y. KIM, J. W. LEE and K. D. SUH, *Macromol. Rapid. Commun.* **22** (2001) 1432.

*Received 15 March
and accepted 30 April 2002*